

RESEARCH ARTICLE

# Dynamic electrostatic charge of lactose-salbutamol sulphate powder blends dispersed from a Cyclohaler<sup>®</sup>

Susan Hoe, Paul M. Young, and Daniela Traini

Advanced Drug Delivery Group, Faculty of Pharmacy, University of Sydney, Sydney, Australia

## Abstract

**Context:** Electrostatic forces have been claimed to be a mechanism for aerosol deposition in the lungs. However, the extent of its influence on aerosol performance is not clear, particularly for carrier-drug formulations.

**Objectives:** To prepare lactose-salbutamol powder blends, varying in blend ratio, and identify any relationships between salbutamol dose, electrostatic characteristics and *in vitro* aerosol performance.

**Methods:** Decanted lactose and micronized salbutamol sulfate was mixed to produce five blends (equivalent to 50, 100, 200, 300 and 400 µg salbutamol per 33 mg of powder). 33 ± 1 mg of a blend was loaded into a Cyclohaler<sup>™</sup> and dispersed into the electrical Next Generation Impactor (eNGI) at an air flow rate of 60 L/min. This was conducted in triplicate for all five lactose-salbutamol blends.

**Results:** Fine particle fraction increased with salbutamol dose, from 5.89 ± 1.42 to 21.35 ± 2.91%. Specific charge (charge divided by mass) distributions for each blend were greatest in magnitude for the 50 µg blend and similar in magnitude between all other blends. However, in eNGI Stage 1 (>8.06 µm), specific charge decreased from 100 µg (−170.4 ± 45.8 pC/µg) to 400 µg (−10.0 ± 9.1 pC/µg).

**Conclusions:** The improvement in fine particle fraction with increased salbutamol dose was indicative of fine drug binding to high and low energy sites on the lactose carrier surface. This finding was supported by electrostatic charge results, but the aerosol charge itself was not found to influence aerosol performance by electrostatic forces.

**Keywords:** Electrostatic charge, lactose, carrier, salbutamol sulfate, eNGI

## Introduction

Binary formulations have been explored as a method for delivering small doses of fine active pharmaceutical ingredient (API) into the respiratory system. The current understanding is that blending an API with large carrier particles aids in dose reproducibility and powder flow during manufacture (by uniformly “coating” the carrier particle with fine drug particles)<sup>1,2</sup>. However, this means that the API must firstly detach from the carrier, and then deaggregate, in order to reach the lungs during inhalation. Factors that may affect the detachment of fines include carrier morphology<sup>1,3</sup>, surface energy<sup>2,4-6</sup> and relative humidity<sup>7</sup>.

Electrostatic forces may also play a role in aiding or hindering API dispersion, but this has yet to be extensively explored. There have been two *in vivo* studies

which have investigated the relationship between particle charge and human lung deposition using carnauba wax particles and found total lung deposition to increase when charged aerosols were inhaled by the test subjects, in comparison with neutral aerosols<sup>8,9</sup>. These results were attributed to the induction of image charge on airway walls, which produced an attractive force that facilitated particle deposition. However, these studies employed particles with a controlled magnitude of charge imparted to them by a corona charger.

The study of triboelectrification (charging through surface contact), generated during the dispersion of medicinal aerosols under inhalational airflow, is of interest as it may provide information about the magnitude of electrostatic charge carried by aerosol particles after release from an inhaler device. Measurement of aerosol charge

Address for Correspondence: Paul M. Young, Advanced Drug Delivery Group, Faculty of Pharmacy, University of Sydney, Sydney NSW 2006, Australia. Tel.: +61 2 90367035. Fax: +61 2 93514391. E-mail: paul.young@sydney.edu.au

(Received 22 November 2010; revised 25 March 2011; accepted 28 March 2011)

could indicate whether electrostatic forces influence particle deposition. Investigations of electrostatic charge in medicinal aerosols have been limited to *in vitro* studies, which have involved a range of apparatuses. Apparatuses specifically used to test dry powder formulations have included the Faraday well<sup>10,11</sup>, aerosol electrometer<sup>12</sup> and electrical low-pressure impactor (ELPI)<sup>7,13-16</sup>.

The electrical Next Generation Impactor (eNGI) has been used by the authors to determine the electrostatic characteristics of Ventolin<sup>TM</sup><sup>17</sup>, QVAR<sup>TM</sup><sup>17</sup>, Flixotide<sup>TM</sup><sup>17,18</sup> and Seretide<sup>TM</sup><sup>18</sup> commercial pressurized metered dose inhalers (pMDIs), as well as Pulmicort<sup>TM</sup> and Bricanyl<sup>TM</sup> Turbuhaler dry powder inhalers<sup>19</sup>. The NGI (from which the eNGI was constructed) can be fitted with a pre-separator for the collection of large particles and is approved for use in the compendia across the air flow rates of 30 to 100 L/min<sup>20</sup>.

Compared to a drug-only formulation, the electrostatic characteristics of a carrier-drug binary formulation include the triboelectric charge of the detached fines as well as that of the carrier particles and undetached fines. Although there have been studies which have looked at the dynamic charge (triboelectrification during dispersion of particles under airflow) of lactose carrier-drug blends, most have either only measured the charge of detached fine particles<sup>15,21</sup> or have not separated carrier particles from the aerosol cloud during powder dispersion into an impactor<sup>7</sup>. The eNGI has been updated from the design described in existing publications<sup>17-19</sup>, to add charge measurement capabilities to the NGI pre-separator and USP induction port, allowing for differentiation in the aerosol charges of fine and coarse particles<sup>22</sup>.

The current evidence for the effect of blend dynamic charge on drug delivery to the lungs is inconclusive. Young et al.<sup>7</sup> proposed a reduction in surface charge on salbutamol and lactose particles as the cause of improved fine particle fraction (FPF) between storage humidities of 0 and 60% relative humidity (RH). Other studies of lactose-salbutamol blend dynamic charge by Telko et al.<sup>15</sup> and Zhu et al.<sup>23</sup> did not speculate on the relationship between delivered dose and specific charge.

However, previous work by Hoe et al.<sup>22</sup> showed that increased flow rate from 30 to 90 L/min increased FPF of a 67.5:1 (% w/w) lactose carrier-salbutamol blend, without a corresponding change in fine particle specific charge. It is possible that the mechanism of charge separation (where a net charge is split across two contacting surfaces into net positive and net negative charge), during fine drug detachment from the carrier surface, would have a greater impact on aerosol performance than changes in tribocharging with increased flow rate. One way to investigate charge separation is to study a variety of carrier-drug blend ratios.

The aim of the current study is to employ the updated eNGI to examine the electrostatic characteristics of a range of lactose carrier-salbutamol sulfate powder blends which differ in carrier-to-drug ratio, assess the relationship between salbutamol sulfate dose and fine particle

deposition and determine if electrostatic charge has a mechanistic influence on *in vitro* aerosol performance.

## Materials and methods

### Materials

Salbutamol sulfate was acquired from S & D Chemicals (Sydney, Australia), whereas  $\alpha$ -lactose monohydrate was supplied by Friesland Foods Domo (Zwolle, Netherlands). high performance liquid chromatography (HPLC)-grade methanol (Sigma-Aldrich, St Louis, MO) and sodium dodecyl sulfate (Mallinckrodt Baker, Phillipsburg, NJ) were used as received.

### Preparation of lactose carrier particles and micronized salbutamol sulfate

A batch of 63–90  $\mu$ m lactose carrier particles was produced by dry sieving 450 g of  $\alpha$ -lactose monohydrate through a nest of sieves (Endecotts Ltd., UK) in a sieve shaker (Vibro Retsch, Haan, Germany). This 63–90  $\mu$ m sieve fraction was subsequently dispersed in lactose-saturated ethanol, sonicated for 5 min and stirred with a spatula to form a homogeneous suspension. After settling, the supernatant was decanted and replaced with fresh lactose-saturated ethanol.

The above dispersion and decantation procedure was repeated until the supernatant was clear. The settled lactose (referred to as decanted lactose in this manuscript) was recovered and dried in a vacuum oven (Weiss-Gallenkamp, Loughborough, UK) at 65°C, before storage in a polypropylene container with silica gel until required.

Salbutamol sulfate was micronized with an air jet mill (Trost Air Impact Pulveriser, Trost Equipment Corporation, Newtown, Philadelphia) at a feed pressure of 280 kPa and grinding pressure of 680 kPa.

### Particle sizing of lactose carrier and micronized salbutamol sulfate

The particle size distributions (PSD) of lactose carrier and salbutamol sulfate were measured using the Malvern Mastersizer 2000 (Malvern Instruments, Worcestershire, UK). For lactose, the Hydro2000SM wet dispersion cell was installed. The lactose was dispersed in a chloroform-filled small volume sample presentation unit, using a dispersion unit controller at a stirrer speed of 2000 rpm. Particle size measurements (in triplicate; refractive indices were 1.444 for chloroform, 1.533 for lactose) produced a distribution of  $d_{10}$ =61.63  $\mu$ m,  $d_{50}$ =98.66  $\mu$ m and  $d_{90}$ =154.95  $\mu$ m, with 1.27% of the powder smaller than 5  $\mu$ m in diameter.

The PSD of micronized salbutamol sulfate (with the Scirocco 2000 dry dispersion unit installed; refractive index of 1.52 for salbutamol sulfate) was  $d_{10}$ =0.81  $\mu$ m,  $d_{50}$ =1.73  $\mu$ m and  $d_{90}$ =3.53  $\mu$ m.

### Preparation of lactose-salbutamol sulfate blends

The five blends to be tested in this study contained drug-to-lactose ratios of 1:659, 1:329, 1:164, 1:109 and 1:81.5

(equivalent to a salbutamol sulfate dose of 50, 100, 200, 300 and 400 µg per 33 mg of powder). Each blend was prepared by geometric hand mixing, before transfer into a glass vial (20 mL volume) and mixing in a Turbula Mixer (Basel, Switzerland) for 15 min, at a speed of 46 revolutions per minute.

The prepared blend was subsequently deionized with a Zerostat 3 anti-static gun (Milty, Hertfordshire, UK) and stored in a container with silica gel for 1 week to allow for charge relaxation. For the remainder of this article, the blends will be referred to by the amount of salbutamol sulfate contained in a single 33 mg powder dose (e.g. the 1:659 blend is the "50 µg blend").

### Updated setup of the eNGI

Previous publications involving the eNGI have only been concerned with the measurement of net charge within the impaction stages<sup>17-19</sup>. The setup of the eNGI has been described in the aforementioned publications, but to summarize, an NGI (Copley Scientific, UK) is enclosed within an earthed steel cage as a shield from environmental interference, while each impaction stage is electrically isolated from adjacent stages and the impactor body with polytetrafluoroethylene (PTFE). The USP induction port, pre-separator and NGI body are isolated with polypropylene adaptors. Consequently, each isolated section behaves as an individual Faraday well.

An electrometer probe (constructed from BNC plugs and quad-shielded coaxial cables) conducts current from its point of contact with an isolated section toward a multichannel electrometer (Keithley 6517A electrometer with 6521 10-channel scanner card; Keithley Instruments, Cleveland, OH). The eNGI design has been revised by Hoe et al.<sup>22</sup> to facilitate additional charge measurement from the USP induction port and pre-separator (Figure 1). A total of 10 probes conduct current from the eNGI sections toward the 10 channels within the electrometer. The

electrometer records data from all 10 channels in succession to complete a scan and was set to operate at 1 scan/sec. Current-versus-time data from all channels are collected by a PC, via serial communication. The NGI outlet is connected to a Busch R5 0025 rotary vane vacuum pump (Busch, Germany).

### Procedures before, during and after eNGI measurement

The following procedure applies for each measurement. The vacuum pump airflow rate was adjusted to 60 L/min with a calibrated mass flowmeter (TSI Model 4040, TSI Instruments, Germany). The eNGI impaction plates were coated with 1% (v/v) silicone/hexane solution and the solvent was left to evaporate. 15 mL of deionized and purified water was placed in the pre-separator well.  $33 \pm 1$  mg of the desired powder blend was filled into a size-3 gelatin capsule, loaded into a Cyclohaler™ device, and attached to the USP induction port. The electrometer baseline was zeroed, and vacuum airflow was initiated for 4 sec, thus completing a single dispersion of powder. After each dispersion, the Cyclohaler™, capsule, induction port and eNGI impaction stages were each rinsed with 5 mL of deionized and purified water. Dispersions were carried out in triplicate. Environmental conditions during the dispersions were  $46.5 \pm 1.6\%$  RH and  $20.1 \pm 2.4^\circ\text{C}$  ( $n=5$ ). All samples were subjected to mass assay by HPLC.

### HPLC

The HPLC setup was a Shimadzu Prominence UFLC system containing an SPD-20A UV-Vis detector, LC-20AT liquid chromatograph, RID 10A refractive index detector and SIL-20A HT Autosampler (Shimadzu Corporation, Japan). Detection of salbutamol sulfate required a mobile phase mixture of 60:40 (% v/v) methanol:water solution and 1 g/L sodium dodecyl sulfate, Waters Nova-Pak C18 4 µm  $3.9 \times 150$  mm column

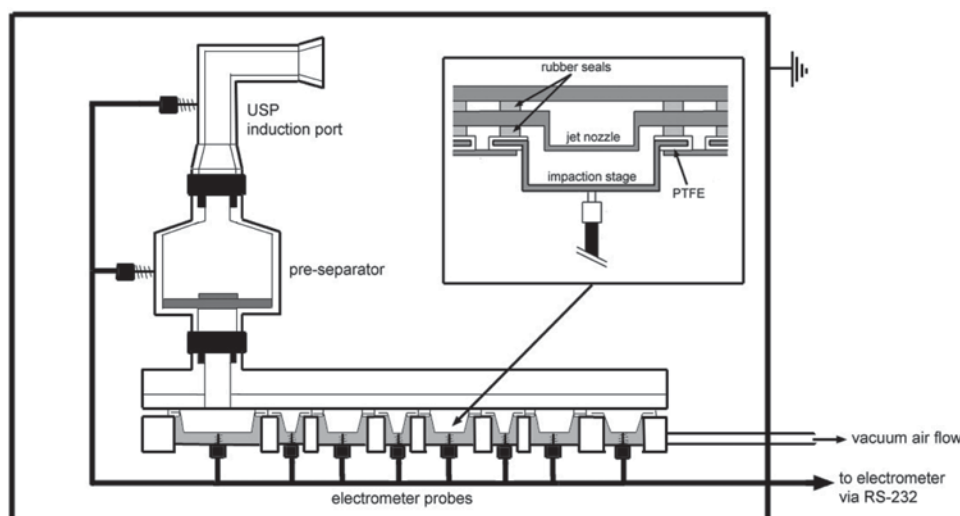


Figure 1. Schematic diagram of the electrical Next Generation Impactor (eNGI) setup. Additional probes have been connected to the pre-separator and USP induction port to provide charge measurement capabilities to these regions.

(Waters Corporation, Milford, MA), mobile phase flow rate of 1 mL/min, UV detection at 276 nm and an injection volume of 100  $\mu$ L.

Lactose detection required a mobile phase of 100% deionized water, with a Waters Resolve C18 5  $\mu$ m 3.9  $\times$  150 mm column (Waters Corporation). Mobile phase flow rate was 1 mL/min, refractive index detection was used, and the injection volume was 100  $\mu$ L.

### Dose content uniformity tests

Ten doses ( $33 \pm 1$  mg) of each carrier-drug blend were assayed by HPLC. The mass of salbutamol sulfate in each dose, for all blends, were within 85 to 115% of the average content, thus satisfying compendial requirements for dose content uniformity<sup>20,24</sup>.

### Data processing and statistical analysis

Current-versus-time data from each electrometer channel was integrated to produce a calculation of net charge per stage according to the following equation:

$$Q = It \quad (1)$$

where  $Q$  is the charge in coulombs (C),  $I$  is the current in amperes (A), and  $t$  is the time in seconds (s). The net charge was also divided by the total mass (lactose and salbutamol sulfate) deposited in that stage to obtain the net charge / mass ratio (referred to as *specific charge* for the remainder of the article). By correcting charge for powder mass, we may get a further idea about the difference in triboelectrification between lactose-salbutamol blends.

*Fine particle dose* (FPD) is defined in this study as the cumulative mass of API with an aerodynamic diameter less than 5  $\mu$ m; it is calculated from linear regression of a cumulative mass versus log cut-off diameter plot, which is graphed for each dispersion. *Recovered dose* (RD) was defined as the total drug collected after mass assay; emitted dose (ED) was total mass deposited outside of the Cyclohaler<sup>TM</sup> and capsule; and FPF was determined as FPD divided by RD. The mass balance for salbutamol sulfate recovered per dispersion was calculated as a percentage of the total weighed drug in the corresponding blend. The total weighed salbutamol per 33 mg blend was estimated from the mass of weighed blend and blend ratio. Statistical analysis of all aerosol performance parameters (FPD, FPF, RD and ED) were subjected to ANOVA one-way analysis (significant difference between pairs when  $p < 0.05$ ) with the SPSS 17.0 statistical analysis package (SPSS Inc., Chicago, IL).

### Scanning electron microscopy

A sample from each of the prepared carrier-drug blends were imaged with scanning electron microscopy using the Philips XL-30 SEM (Philips, Germany) to observe the distribution of salbutamol particles on the decanted lactose surface.

## Results

### Mass deposition of lactose and salbutamol sulfate

No lactose was detected in the eNGI impaction stages. The mass deposition of lactose carrier from each blend in the Cyclohaler<sup>TM</sup>, USP induction port and pre-separator is presented in Figure 2, expressed in terms of percentage deposition (lactose mass divided by recovered mass). Between the 100  $\mu$ g and 400  $\mu$ g blends, the distribution within this region of the eNGI showed an increase in USP induction port deposition ( $5.1 \pm 1.3$  to  $20.9 \pm 7.1\%$ ) and a decrease in pre-separator deposition ( $94.1 \pm 1.4$  to  $78.2 \pm 7.0\%$ ), although the 200 and 300  $\mu$ g blends do not follow this trend.

The mass deposition of salbutamol sulfate in the Cyclohaler<sup>TM</sup>, USP induction port and pre-separator increased with salbutamol dose per blend, from 50  $\mu$ g to 400  $\mu$ g—from  $1.24 \pm 0.13$  to  $39.29 \pm 0.98$   $\mu$ g in the Cyclohaler,  $3.59 \pm 0.98$  to  $68.78 \pm 4.89$   $\mu$ g in the USP induction port and  $44.26 \pm 2.63$   $\mu$ g to  $184.70 \pm 3.60$   $\mu$ g in the pre-separator. Percentage deposition of salbutamol sulfate was also calculated (salbutamol mass divided by recovered mass) and shown in Figure 3A. The distribution of the 50  $\mu$ g blend is distinct from the rest, with  $2.2 \pm 0.2\%$  collected from the Cyclohaler<sup>TM</sup> and  $6.4 \pm 1.9\%$  from the USP induction port, both significantly less than all other blends. Meanwhile,  $79.09 \pm 3.52\%$  was deposited in the pre-separator and  $4.11 \pm 0.85\%$  in Stage 1 ( $>8.06$   $\mu$ m), both significantly greater than all other blends. A comparison between 100, 200, 300 and 400  $\mu$ g blends showed no difference in device retention. From 100 to 400  $\mu$ g, there was a small increase in percentage deposition in the USP induction port and a general decrease in percentage deposition within the pre-separator.

The PSD of salbutamol sulfate corresponding to dose are shown in Figure 3B. Peak deposition in the eNGI impaction stages increased with salbutamol sulfate dose. Table 1 is a summary of the *in vitro* aerosol parameters FPD, ED, RD and FPF, calculated for salbutamol. An increase in salbutamol dose corresponded with an increase in ED ( $49.98 \pm 7.81$  to  $349.47 \pm 19.83$   $\mu$ g), FPD ( $3.29 \pm 0.79$  to  $83.37 \pm 15.24$   $\mu$ g), RD ( $55.93 \pm 1.04$  to  $388.76 \pm 20.12$   $\mu$ g) and FPF ( $5.89 \pm 1.42$  to  $21.35 \pm 2.91\%$ ). One-way ANOVA statistical analysis identified a statistically significant difference ( $p < 0.05$ ) in FPF, between 50  $\mu$ g and all other blends, 100  $\mu$ g and 300  $\mu$ g blends, and 100  $\mu$ g and 400  $\mu$ g blends.

Mass balance of salbutamol for each blend is shown in Table 1, ranging from 90% for the 100  $\mu$ g blend to 98% for the 50 and 300  $\mu$ g blends. One-way ANOVA statistical analysis showed no statistically significant difference between all the blends. The SEM images for each of the blend are shown in Figure 4.

### Net charge distribution results

Table 2 shows the net charge (in nC) and specific charge (in nC/mg) of the lactose-salbutamol blends deposited



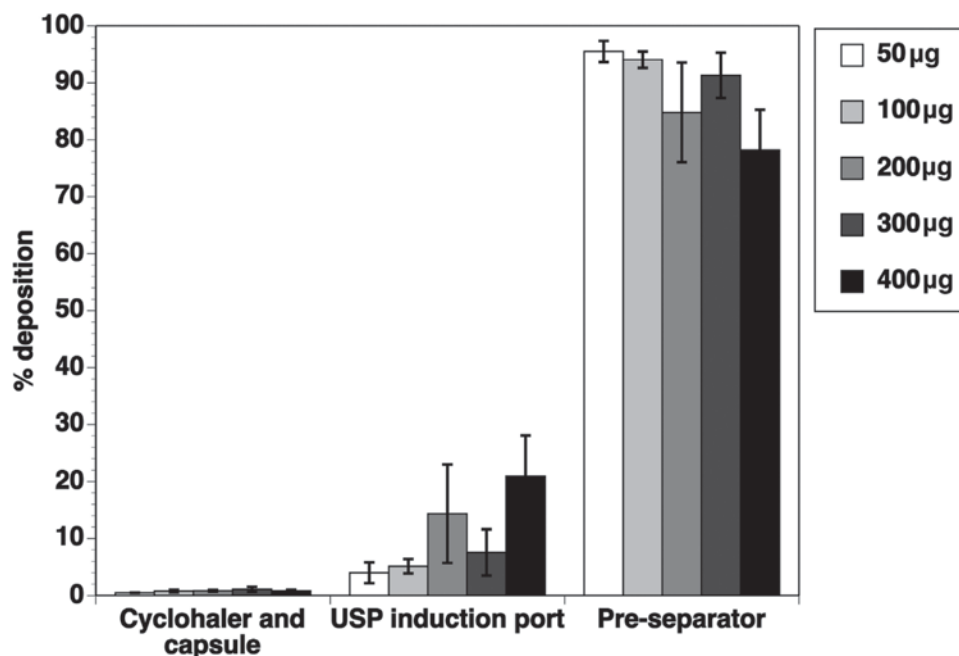


Figure 2. Percentage deposition of lactose in the Cyclohaler™, USP induction port and pre-separator after dispersion of lactose-salbutamol blend (expressed as salbutamol dose per 33 mg of powder) from a Cyclohaler™ into the electrical Next Generation Impactor (eNGI) at 60 L/min ( $n=3$ , mean  $\pm$  SD).

in the USP induction port and pre-separator. In addition, the charge polarity of each dispersion is reported. Within the USP induction port, dispersions were both net negative and net positive, and, as a result, the errors are very large and there is no discernible trend in net charge according to blend. This phenomenon has been reported previously<sup>22</sup> and is thought to be the result of current in the airflow (varying between +4 and -4 nA), induced by triboelectrification of a rapidly oscillating gelatin capsule in the Cyclohaler™ during dispersion.

Meanwhile, dispersions were uniformly net negative in polarity within the pre-separator. This result is also consistent with findings by Hoe et al.<sup>22</sup>. Net charge in the pre-separator appears to increase from the 50 µg blend ( $-5.99 \pm 1.03$  nC) to 200 µg blend ( $-9.64 \pm 0.83$  nC) and decrease from the 200 µg blend to 300 µg blend ( $-2.84 \pm 2.42$  nC).

Specific charge in the USP induction port and pre-separator requires the division of net charge by the total lactose and salbutamol sulfate mass recovered within the region. As with net charge alone, no trend according to blend was observed within the USP induction port as the large errors in net charge were simply carried over. However, specific charge in the pre-separator generally decreased from 50 µg ( $-0.22 \pm 0.06$  nC/mg) to 400 µg ( $-0.15 \pm 0.08$  nC/mg), although the only statistically significant difference in mean values was found between 100 and 300 µg (one-way ANOVA,  $p < 0.05$ ).

The net charge distributions of salbutamol sulfate fines in the impaction stages are shown in Figure 5. There appears to be two sections of net negative charge—within Stage 1 ( $>8.06$  µm) and between Stages 3 and 6 ( $0.55$ – $2.82$  µm). In the latter region, net charge

increases from the 50 µg blend to 400 µg blend, although there is considerable overlap between 50 and 100 µg, and between 200, 300 and 400 µg. In comparison, within Stage 1, net charge decreases from 50 µg to 400 µg, although once again the variation in charge results in significant overlap.

The mean specific charge distributions of salbutamol sulfate doses within the impaction stages are shown in Figure 6. Unlike the net charge distributions in Figure 5, the 50 µg blend distribution is distinctly greater in magnitude than those of other doses, which extensively overlap. In Stage 1, there is a decrease in charge / mass ratio from 100 µg ( $-170.4 \pm 45.8$  pC/µg) to 400 µg ( $-10.0 \pm 9.1$  pC/µg); however, 50 µg ( $-115.5 \pm 60.9$  pC/µg) sits in between 100 and 200 µg.

## Discussion

### Coarse particle deposition

There has been discussion about how ternary fine particles, such as lactose fines, aid the dispersion of drug from a carrier-drug blend. One theory proposes that the lactose carrier particle possesses regions of high and low binding energy. The attachment of lactose fines to the high-energy regions prevent the fine drug particles from binding to these areas, thus allowing them to detach more easily during aerosolization. Another hypothesis proposes that lactose fines form multiplets with fine drug particles, which detach more easily from the lactose carrier than fine drug alone<sup>25,26</sup>.

In this study, lactose carrier particles were subjected to the wet decantation method, which removed the majority of lactose fines from its surface. In doing so, high energy

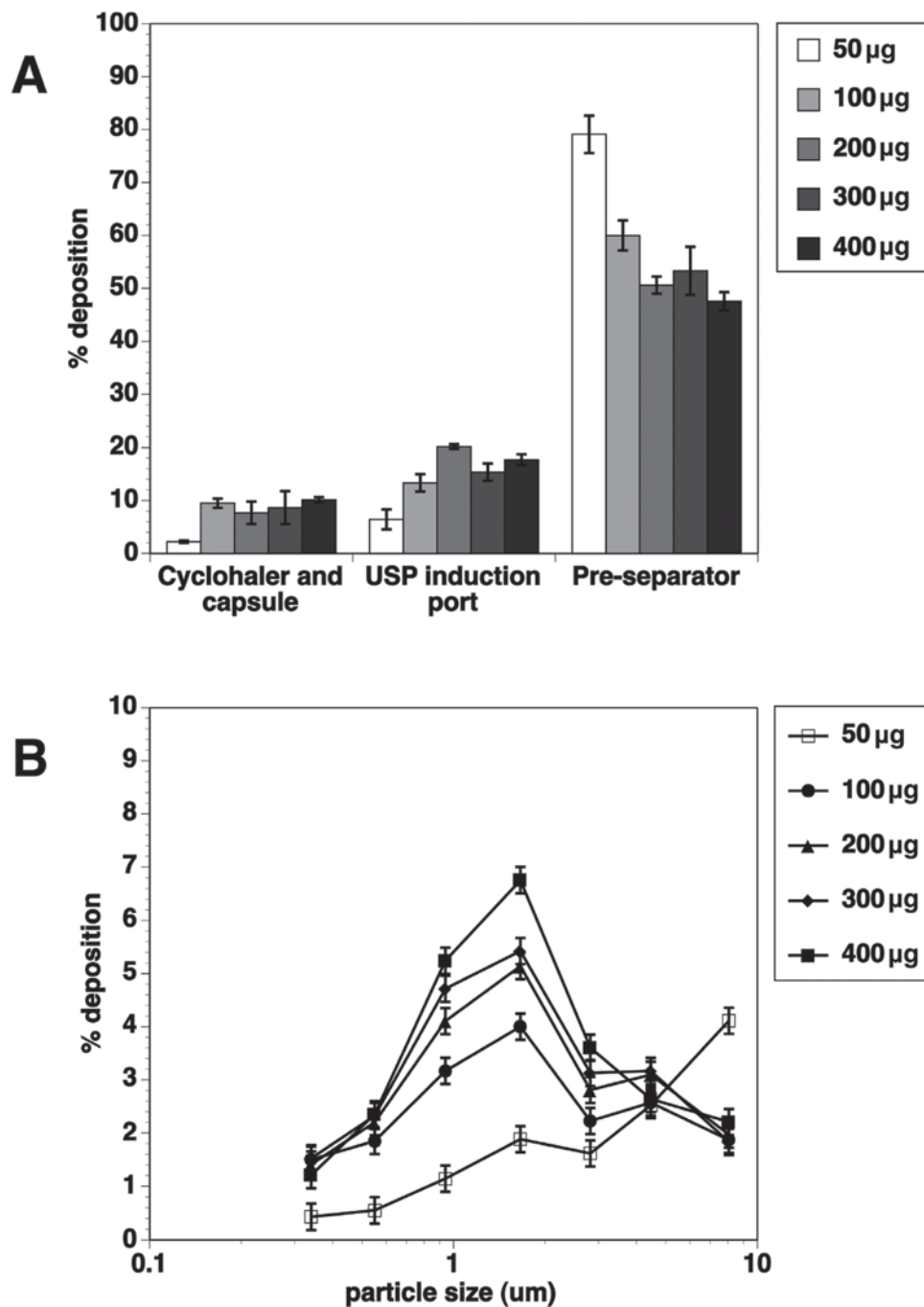


Figure 3. Percentage deposition of salbutamol sulfate into the Cyclohaler™, USP induction port, pre-separator (A) and in the electrical Next Generation Impactor (eNGI) impaction stages (B), according to lactose-salbutamol sulfate blend (expressed as salbutamol dose per 33 mg of powder).

Table 1. Mean *in vitro* aerosol parameters calculated for lactose-salbutamol blends (containing 50 to 400 µg salbutamol per 33 mg powder), after dispersion from a Cyclohaler™ into the electrical Next Generation Impactor (eNGI) at 60 L/min ( $n=3$ , mean  $\pm$  SD).

	Blend (µg salbutamol sulfate per 33 mg)				
	50	100	200	300	400
Emitted dose (ED, µg)	50.0 $\pm$ 7.8	82.1 $\pm$ 9.4	181.1 $\pm$ 3.5	281.1 $\pm$ 29.1	349.5 $\pm$ 19.8
Fine particle dose (FPD, µg)	3.3 $\pm$ 0.8	12.3 $\pm$ 0.9	34.4 $\pm$ 1.5	58.1 $\pm$ 7.7	83.4 $\pm$ 15.2
Recovered dose (RD, µg)	55.9 $\pm$ 1.0	90.7 $\pm$ 9.5	196.2 $\pm$ 4.7	307.9 $\pm$ 33.8	388.8 $\pm$ 20.1
Mass balance (%)	97.4 $\pm$ 1.2	90.4 $\pm$ 9.6	97.7 $\pm$ 4.1	94.9 $\pm$ 6.7	95.9 $\pm$ 5.1
Fine particle fraction (FPF, %)	5.9 $\pm$ 1.4	13.6 $\pm$ 1.9	17.6 $\pm$ 1.2	18.9 $\pm$ 1.7	21.4 $\pm$ 2.9

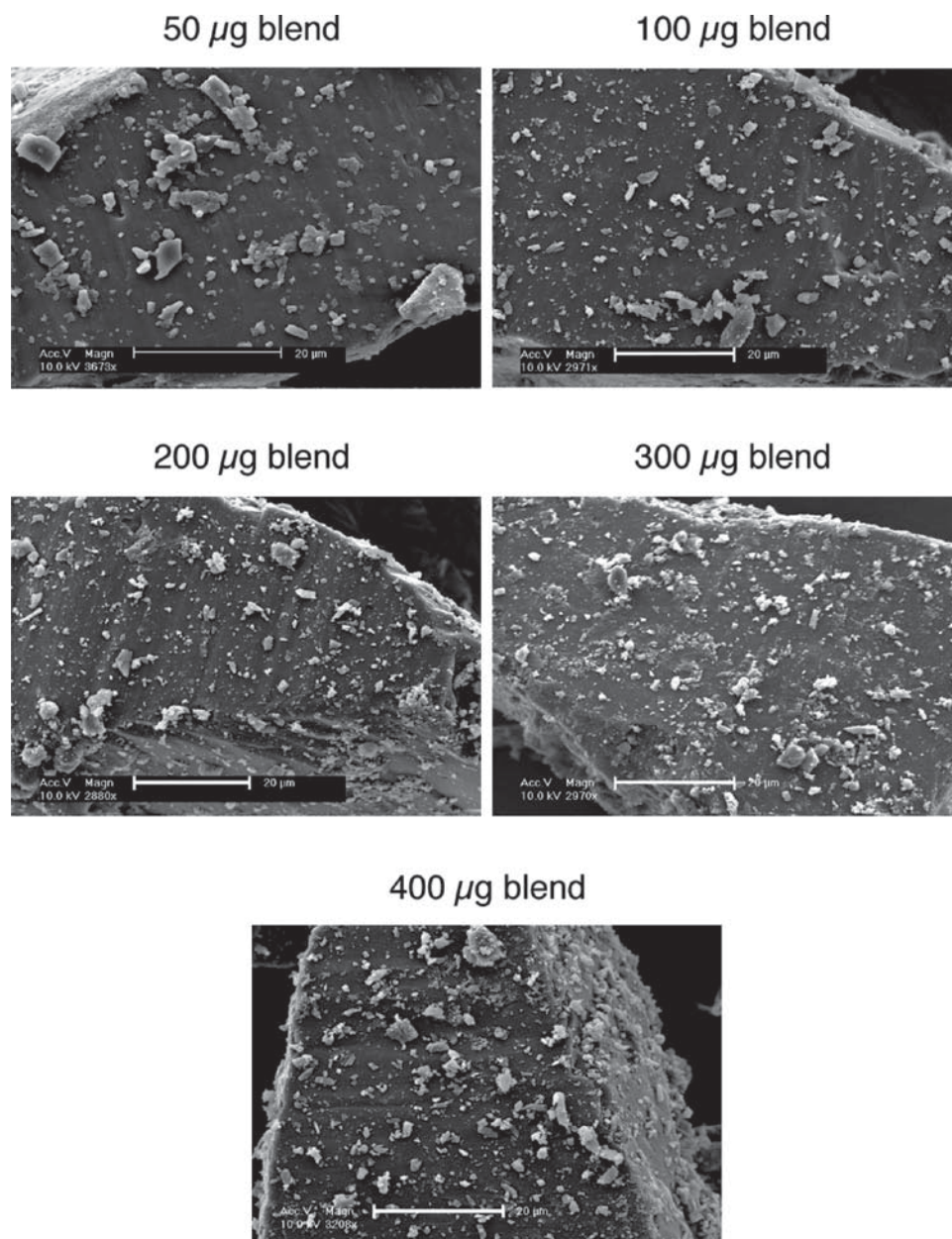


Figure 4. SEM images of 63–90  $\mu\text{m}$  decanted lactose carrier particles from the 50, 100, 200, 300 and 400  $\mu\text{g}$  blends. The scale bars are equivalent to 20  $\mu\text{m}$ .

Table 2. Mean net charge (nC) and specific charge (nC/mg) measured in the USP induction port and pre-separator for lactose-salbutamol blends (containing 50 to 400  $\mu\text{g}$  salbutamol per 33 mg powder), after dispersion from a Cyclohaler™ into the electrical Next Generation Impactor (eNGI) at 60 L/min ( $n=3$ , mean  $\pm$  SD). The charge polarity measured from each dispersion is also shown.

Salbutamol sulfate dose ( $\mu\text{g}$ )	Net charge (nC)		Specific charge (nC/mg)	
	USP induction port	Pre-separator	USP induction port	Pre-separator
50	$2.37 \pm 1.27$ +,+,+	$-5.99 \pm 1.03$ -,-,-	$2.58 \pm 1.96$	$-0.22 \pm 0.06$
100	$1.32 \pm 4.83$ +,+,-	$-6.92 \pm 0.94$ -,-,-	$1.19 \pm 3.40$	$-0.25 \pm 0.02$
200	$0.94 \pm 0.40$ -,+,+	$-9.64 \pm 0.83$ -,-,-	$-0.04 \pm 0.16$	$-0.19 \pm 0.03$
300	$1.95 \pm 0.36$ +,+,+	$-2.84 \pm 2.42$ -,-,-	$1.02 \pm 0.38$	$-0.11 \pm 0.09$
400	$-0.49 \pm 0.93$ +,-,+	$-3.71 \pm 2.23$ -,-,-	$-0.06 \pm 0.11$	$-0.15 \pm 0.08$

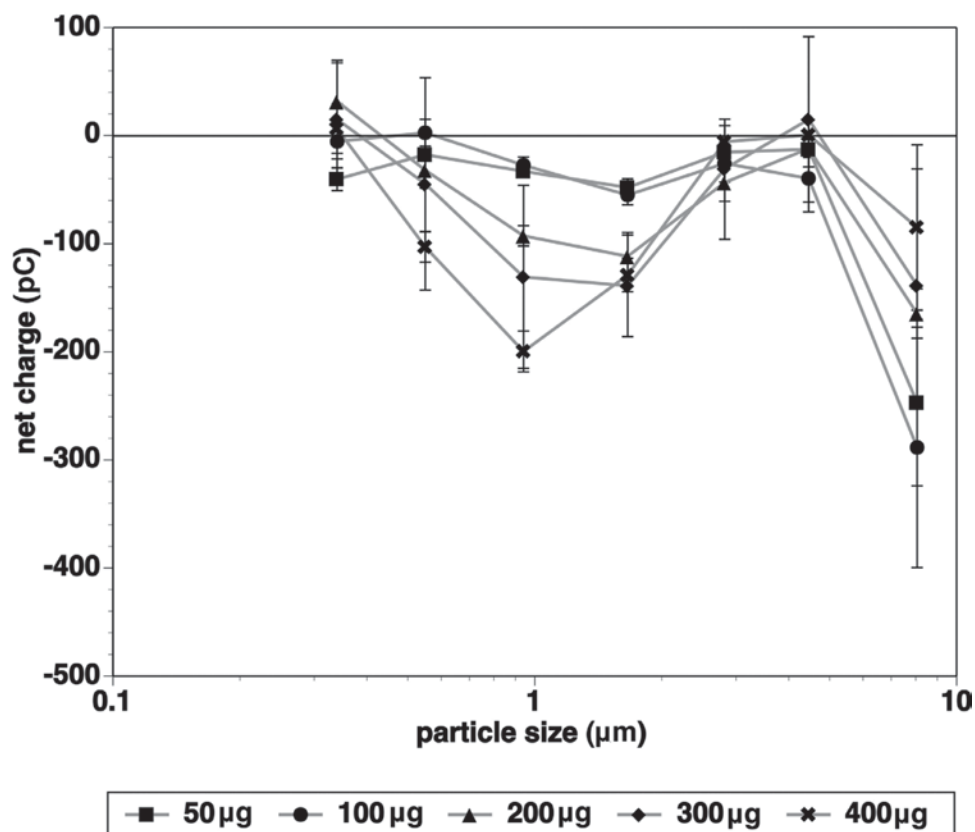


Figure 5. Net charge (pC) distributions of salbutamol corresponding to particle size, after dispersion of lactose-salbutamol blend (expressed as the salbutamol dose per 33 mg of powder) into the electrical Next Generation Impactor (eNGI) at 60 L/min ( $n=3$ , mean  $\pm$  SD).

binding sites may have become exposed to interaction with fine salbutamol sulfate. As the amount of salbutamol sulfate blended with decanted lactose is increased, these sites would eventually saturate with drug, and additional salbutamol above this saturation concentration would be bound to low energy binding sites.

The consequence of this may be observed in the percentage deposition of lactose and salbutamol in the pre-separator (Figures 2 and 3A). 50 to 80% salbutamol deposited in the pre-separator, compared to 75 to 95% lactose within the same region. This reflects the detachment of drug particles from the lactose carrier. Meanwhile, percentage deposition of salbutamol decreased from 80 to 60% between 50 and 100  $\mu$ g blends and levelled out at 50% for 200 to 400  $\mu$ g blends. This can be explained by the saturation of high energy binding sites on lactose carrier particles, shown in Figure 6. At a 50  $\mu$ g dose, the high energy binding sites have not yet been fully occupied by fines (both lactose and drug), leading to disproportionally poor dispersion of salbutamol sulfate. At 100  $\mu$ g dose, high energy binding sites are almost completely occupied, and with doses of 200  $\mu$ g and above, these sites are fully occupied, and percentage deposition of salbutamol sulfate in the pre-separator has levelled off as a result.

Given that crevices in the carrier surface are prime candidates for high energy binding sites, surface roughness may be an indicator of how much fine particles

are required before the high energy regions are wholly occupied. The surface of the decanted lactose carrier shows signs of etching (Figure 4), similar to the 5% surface-dissolved lactose prepared by El-Sabawi et al.<sup>3</sup>. It is possible that some surface smoothing has occurred with the 63–90  $\mu$ m decanted lactose in this study, reducing the number of high energy binding sites and, thus, also reducing the salbutamol concentration at which saturation of high energy binding sites is achieved.

The inconsistency in charge polarity within the USP induction port (Table 2) is the consequence of charge manifested from the rubbing of gelatin capsule against the surface. A previous study conducted by the authors found that tribocharging of an empty gelatin capsule in a Cyclohaler™, during dispersion under vacuum airflow, led to discharge in air—detected only in the USP induction port and pre-separator<sup>22</sup>. The current detected in these regions oscillated over time between net positive and negative charge and were of such great magnitude in the USP induction port ( $\pm 4$  nA) that the subsequent measurement of aerosol charge from lactose-drug blends was affected. This has also been observed in this study, as the inconsistent charge polarity in the USP induction port has resulted in mean net charge measurements with variations exceeding 100% of the mean (100 and 400  $\mu$ g doses). As a result, USP induction port charge cannot be interpreted to much effect. The use of capsules made from materials other than gelatin would be expected to



generate significant triboelectric charge, given the extensive contact charging between the capsule and inhaler surfaces as the capsule rattles quickly during powder dispersion, and the contacting surfaces of the capsule and inhaler are part of insulating materials.

Whereas the pre-separator net charge increased from 50  $\mu\text{g}$  to 200  $\mu\text{g}$  blends, and declined from 200 to 400  $\mu\text{g}$  blends, the pre-separator specific charge showed a different trend. The lactose mass constituted the vast majority of each dispersed dose ( $33 \pm 1$  mg), and as the lactose mass collected in the pre-separator decreased with increased salbutamol sulfate dose, specific charge should increase

accordingly. However, the 300 and 400  $\mu\text{g}$  blends produced the lowest specific charge results (Table 2). The fine drug charge was found to be net negative in the impaction stages, regardless of dose (Figure 5), indicating that detachment of fine particles from lactose carrier during aerosolization may have resulted in charge separation, leaving the remaining carrier and undetached fines with a lower net negative specific charge. For 50 and 100  $\mu\text{g}$  blends, where the percentage of drug retained in the pre-separator was greater than the other three doses, there was less charge separation and a higher charge/mass ratio as a result.

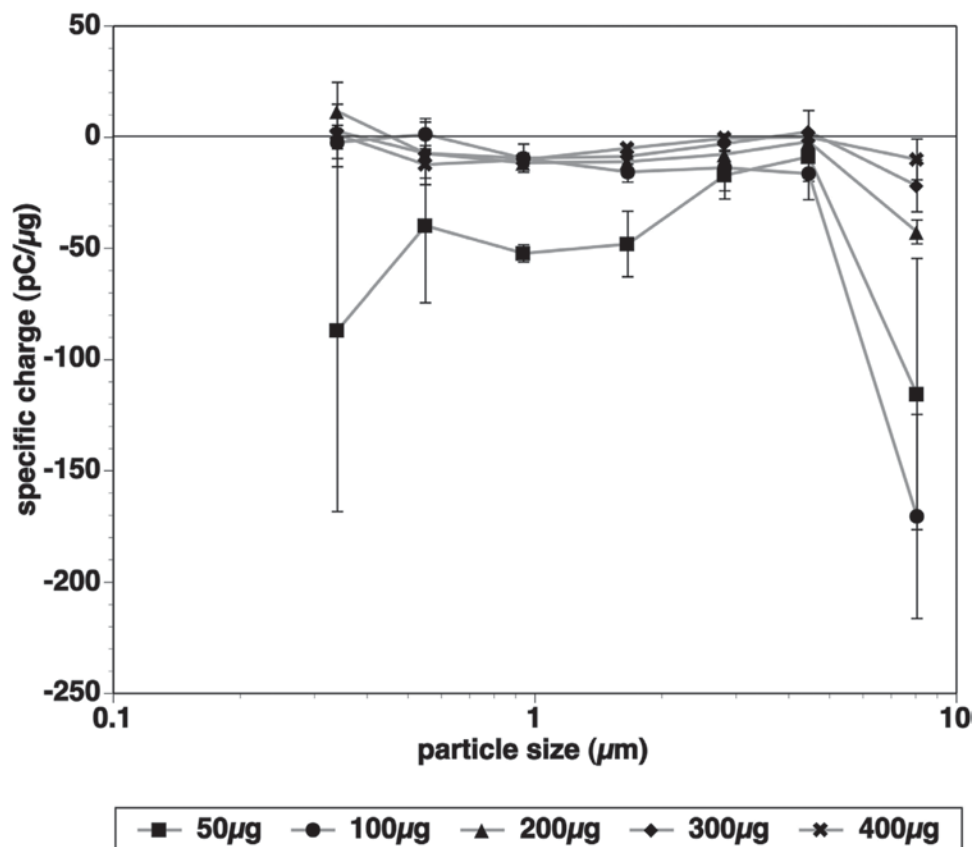


Figure 6. Specific charge (pC/ $\mu\text{g}$ ) distributions of salbutamol corresponding to particle size, after dispersion of lactose-salbutamol blend (expressed as the salbutamol dose per 33 mg of powder) into the electrical Next Generation Impactor (eNGI) at 60 L/min ( $n=3$ , mean  $\pm$  SD).

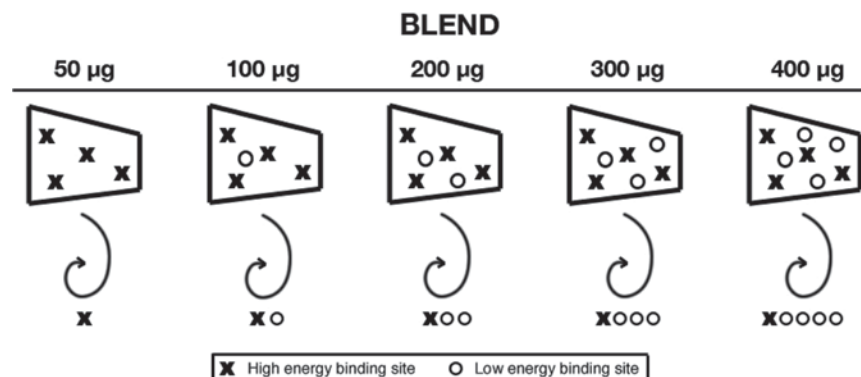


Figure 7. The distribution of fines across the lactose carrier surface and detachment of fines from the carrier surface, corresponding to salbutamol dose, according to the high and low energy binding sites theory.

### Fine particle deposition

The SEM images of the lactose-salbutamol blends (Figure 7) indicate a trend in fines distribution across the lactose surface, according to salbutamol dose. For the 50  $\mu\text{g}$  blend, fines were distributed as a mixture of single particles and multiplets. Within the eNGI impaction stages, the distribution of salbutamol sulfate was different for the 50  $\mu\text{g}$  blend compared to the other powder blends (Figure 3B). At this dose, a significant portion of the salbutamol detached from carrier during dispersion may have been aggregates with an aerodynamic diameter  $>8.06\text{ }\mu\text{m}$ , resulting in  $4.1 \pm 0.8\%$  salbutamol deposited in Stage 1. Meanwhile, only approximately 5.6% of detached salbutamol fines deposited in Stages 3 and below ( $<4.46\text{ }\mu\text{m}$ ).

Following on from the discussion of binding sites in the “Coarse particle deposition” section, the saturation of high energy binding sites with fines within the 50  $\mu\text{g}$  blend suggests that as the salbutamol dose increased, the number of single fine particles and multiplets bound to low energy binding sites also increased (Figure 7). As multiplets may detach more easily from the lactose surface than single particles, a greater percentage of drug can reach the lower impaction stages in the form of primary particles and partly deaggregated fragments. This accounts for the general increase in FPD and FPF with increased salbutamol dose.

The net charge distribution graphs (Figure 5) followed the expected trend of increased charge with salbutamol dose—however, in order to elucidate whether the differences in charge measurement were the result of increased fine particle deposition, or rather the consequence of changing patterns in triboelectrification, the net charge needed to be corrected for mass. Lactose was not detected within these stages; it is possible that the amount present in each stage was below the refractive index limit of detection. As a result, the available net specific charge results were calculated from salbutamol mass alone (Figure 6). Although the specific charge plot for the 50  $\mu\text{g}$  dose appears to be distinctly greater in magnitude than the rest, the mass of salbutamol sulfate is close to, or below, 1  $\mu\text{g}$  in Stages 2–7, effectively distorting the specific charge plot.

Although the specific charge in Stage 1 appears considerably larger than that detected in other impaction stages, its decrease with increasing salbutamol dose from 100 to 400  $\mu\text{g}$  (Figure 6) can be explained in terms of deaggregation and charge separation. As discussed in “Fine particle deposition” section, single particles and multiplets were attached to low energy binding sites in increasing amounts, as salbutamol dose increased. However, it is the multiplets which would be expected to detach more easily from the carrier surface. Consequently, the charge separation mechanism which occurs with agglomerate breakup would also be predicted to have a greater influence with increased salbutamol dose.

Figure 8 depicts a simplified instance of charge separation, where particles previously in contact develop positive or negative charge across the surface during

deaggregation. This results in multiplets or single particles with specific charges different to the original agglomerate. It appears that as salbutamol dose increased, greater multiplet detachment allowed for more deaggregation into primary salbutamol particles, deposited in the lower eNGI stages. Each of the smaller particles seem to have received net negative charge on their detaching surfaces as a consequence of charge separation, and, as a result, net specific charge of the multiplets deposited in Stage 1 continued to decrease, until the 400  $\mu\text{g}$  blend, where net specific charge was comparable to that in the lower stages. However, this is complicated by charge separation between salbutamol and lactose, and the factors that may affect distribution of charge (such as surface area or surface chemistry), making it difficult to fully understand the effect of charge distribution from the specific charge results alone.

The relative humidity of the environment during testing can contribute to the tribocharging process as moisture droplets may aid the transfer of charge from insulating surfaces. As a result, one may predict measured net charge to be greater at low relative humidity. However, as the relative humidity and temperature remained consistent throughout the course of the study, these environmental factors would not have been expected to influence differences in charge between blends.

The specific charge plots for the 100, 200, 300 and 400  $\mu\text{g}$  blends in eNGI Stages 2–7 overlap, which suggests that changes in fine particle fraction were a dominant influence on the changes observed in net charge, over any change in triboelectrification mechanics which occurred concurrently (such as differences in charge separation or surface contact frequency) as salbutamol dose increased. Consequently, from these results, it would appear that net charge is not a strong influencing factor on *in vitro* aerosol performance; rather, the specific charge results serve as supporting evidence for the theory of high and low energy binding sites on carrier particles as well as multiplet fragmentation during aerosol dispersion.

### Conclusions

Aerosolization of low-dose salbutamol sulfate (50  $\mu\text{g}$ ) from 33 mg of a lactose-drug blend produced results distinct to that of other doses (100, 200, 300 and 400  $\mu\text{g}$ ), which can be explained in terms of high and low energy binding sites, and multiplet formation on the lactose carrier surface. Wet decantation exposed high energy sites to binding with

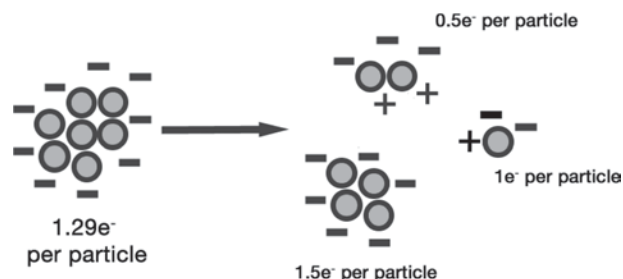


Figure 8. A schematic example of charge separation occurring across contacting particle surfaces during deagglomeration.

drug, affecting drug detachment during aerosolization. As salbutamol dose increased from 50 to 100 µg, these binding sites were eventually occupied, and further increases in dose led to multiplets and single particles attaching to low energy binding sites. During powder dispersion, these more weakly bound particles (multiplets in particular) are detached from the carrier surface. Fine particle fraction for the 50 µg blend was poor as most of the drug was attached to high energy binding sites and less able to detach. As drug dose increased to 400 µg, there was a greater amount of deaggregation into fragments and primary particles, increasing fine particle fraction as a result.

Correction of net charge in the impaction stages for drug mass indicated that from 100 to 400 µg, the magnitude of net charge is directly related to fine particle fraction. The electrostatic characteristics of the lactose-salbutamol blends measured by the eNGI appeared to be secondary to the turbulent and shear forces which aid the detachment of fine particles from the carrier particles.

Decreasing specific charge for the size fraction >8.06 µm with increased dose supports the theory that a greater amount of deaggregation occurred at higher salbutamol doses. The breakdown of aggregates into fragments and primary particles may be accompanied by charge separation; thus, the remaining aggregates which deposit in the uppermost impaction stage carry decreasing specific charge with increased dose.

Although the net charge and specific charge results obtained in this study have not shown an influence on aerosol performance, they have aided further understanding about the mechanisms involved in the attachment of drug to carrier and the dispersion of drug from the carrier.

## Declaration of interest

The authors report no conflict of interest. The authors alone are responsible for the content and writing of the article.

## References

1. Zeng XM, Martin GP, Marriott C, Pritchard J. (2000). The effects of carrier size and morphology on the dispersion of salbutamol sulphate after aerosolization at different flow rates. *J Pharm Pharmacol*, 52:1211-1221.
2. Young PM, Kwok P, Adi H, Chan HK, Traini D. (2009). Lactose composite carriers for respiratory delivery. *Pharm Res*, 26:802-810.
3. El-Sabawi D, Edge S, Price R, Young PM. (2006). Continued investigation into the influence of loaded dose on the performance of dry powder inhalers: surface smoothing effects. *Drug Dev Ind Pharm*, 32:1135-1138.
4. Zeng XM, Martin GP, Marriott C, Pritchard J. (2001). Lactose as a carrier in dry powder formulations: the influence of surface characteristics on drug delivery. *J Pharm Sci*, 90:1424-1434.
5. Saleem I, Smyth H, Telko M. (2008). Prediction of dry powder inhaler formulation performance from surface energetics and blending dynamics. *Drug Dev Ind Pharm*, 34:1002-1010.
6. Traini D, Young PM, Thielmann F, Acharya M. (2008). The influence of lactose pseudopolymorphic form on salbutamol sulfate-lactose interactions in DPI formulations. *Drug Dev Ind Pharm*, 34:992-1001.
7. Young PM, Sung A, Traini D, Kwok P, Chiou H, Chan HK. (2007). Influence of humidity on the electrostatic charge and aerosol performance of dry powder inhaler carrier based systems. *Pharm Res*, 24:963-970.
8. Melandri C, Tarroni G, Prodi V, de Zaiacomo T, Formignani M, Lombardi CC. (1983). Deposition of charged particles in the human airways. *J Aerosol Sci*, 14:657-669.
9. Prodi V, Mularoni A. (1985). Electrostatic lung deposition experiments with humans and animals. *Ann Occup Hyg*, 29:229-240.
10. Murtomaa M, Pekkala P, Kalliohaka T, Paasi J. (2005) A device for aerosol charge measurement and sampling. *J Electrostat*, 63:571-575.
11. Chow KT, Zhu K, Tan RB, Heng PW. (2008). Investigation of electrostatic behavior of a lactose carrier for dry powder inhalers. *Pharm Res*, 25:2822-2834.
12. Byron PR, Peart J, Staniforth JN. (1997). Aerosol electrostatics. I: Properties of fine powders before and after aerosolization by dry powder inhalers. *Pharm Res*, 14:698-705.
13. Glover W, Chan H-K. (2004). Electrostatic charge characterization of pharmaceutical aerosols using electrical low-pressure impactor (ELPI). *J Aerosol Sci*, 35:755-764.
14. Kwok PC, Glover W, Chan HK. (2005). Electrostatic charge characteristics of aerosols produced from metered dose inhalers. *J Pharm Sci*, 94:2789-2799.
15. Telko MJ, Kujanpää J, Hickey AJ. (2007). Investigation of triboelectric charging in dry powder inhalers using electrical low pressure impactor (ELPI). *Int J Pharm*, 336:352-360.
16. Kwok PC, Chan HK. (2008). Effect of relative humidity on the electrostatic charge properties of dry powder inhaler aerosols. *Pharm Res*, 25:277-288.
17. Hoe S, Young PM, Chan HK, Traini D. (2009). Introduction of the electrical next generation impactor (eNGI) and investigation of its capabilities for the study of pressurized metered dose inhalers. *Pharm Res*, 26:431-437.
18. Hoe S, Traini D, Chan HK, Young PM. (2009). The influence of flow rate on the aerosol deposition profile and electrostatic charge of single and combination metered dose inhalers. *Pharm Res*, 26:2639-2646.
19. Hoe S, Traini D, Chan HK, Young PM. (2009). Measuring charge and mass distributions in dry powder inhalers using the electrical Next Generation Impactor (eNGI). *Eur J Pharm Sci*, 38:88-94.
20. United States Pharmacopoeia (USP). Chapter <601>, United States Pharmacopoeia 31 - National Formulary 26: United States Pharmacopoeial Convention Inc.; 2008.
21. Hickey AJ, Mansour HM, Telko MJ, Xu Z, Smyth HD, Mulder T et al. (2007). Physical characterization of component particles included in dry powder inhalers. II. Dynamic characteristics. *J Pharm Sci*, 96:1302-1319.
22. Hoe S, Traini D, Chan HK, Young PM. (2010). The contribution of different formulation components on the aerosol charge in carrier-based dry powder inhaler systems. *Pharm Res*, 27:1325-1336.
23. Zhu K, Ng WK, Shen S, Tan RB, Heng PW. (2008). Design of a device for simultaneous particle size and electrostatic charge measurement of inhalation drugs. *Pharm Res*, 25:2488-2496.
24. British Pharmacopoeia. (2009). Section 2.9.18 - Appendix XII C. Consistency of Formulated Preparations for inhalation.
25. Jones MD, Price R. (2006). The influence of fine excipient particles on the performance of carrier-based dry powder inhalation formulations. *Pharm Res*, 23:1665-1674.
26. Pilcer G, Amighi K. (2010). Formulation strategy and use of excipients in pulmonary drug delivery. *Int J Pharm*, 392:1-19.